An Oceanic Heat Content–Based Definition for the Pacific Decadal Oscillation

ARUN KUMAR

Climate Prediction Center, NOAA/NWS/NCEP, College Park, Maryland

CAIHONG WEN

Climate Prediction Center, NOAA/NWS/NCEP, College Park, and Innovim, Greenbelt, Maryland

(Manuscript received 1 March 2016, in final form 4 August 2016)

ABSTRACT

Based on the variability of heat content in the upper 300 m of the ocean (HC300), the feasibility of defining an index of Pacific decadal oscillation (PDO) is explored. The motivation for defining the PDO index on HC300 stems from the following considerations: (i) a need to accentuate lower-frequency variations in the monitoring of PDO and (ii) to take into account variations in the temperatures associated with the PDO that extend throughout the upper ocean (and are modulated by the seasonal cycle of mixed layer variability). It is demonstrated that an HC300-based definition is better suited to encapsulate these characteristics in the PDO variability. The variability in an HC300-based definition is also contrasted with the traditional definition of the PDO based on SSTs.

1. Introduction

Pacific decadal oscillation (PDO) is one of the dominant modes of sea surface temperature (SST) variability in the North Pacific and has been associated with various biological and physical aspects of variability over this region (Mantua et al. 1997; Liu 2012; Newman et al. 2016). Traditionally PDO has been defined based on the variability associated with SSTs (Mantua et al. 1997; Wen et al. 2014).

Although having a component of variability on a decadal time scale that can either be inferred based on the visual inspection of the SST-based definition of the PDO index (see Fig. 1), or can be quantified based on the spectral analysis (Liu 2012; Wang et al. 2012a), the PDO also has considerable variability on a seasonal time scale. Indeed, the autocorrelation of the SST-based monthly PDO index at 6 months is ~0.6 (Wang et al. 2012a; Wen et al. 2012), indicating that, on average, only 36% of PDO variability later can be explained from its present state. The fast time-scale variation of the traditional PDO index is consistent with the fast time scale of atmospheric variability and the notion that the atmospheric forcing is one of the major contributors for the leading mode of SST variations corresponding to the PDO (Liu 2012; Newman et al. 2016; Kumar and Wang 2015).

Notwithstanding considerable variation on a monthly time scale, the term PDO also conveys the impression that it is a mode with temporal variations on slower time scales (e.g., interannual to decadal). This is in contrast to the high-frequency variability that is inherent in the SST-based index of the PDO. In the paradigm of high-frequency atmospheric variability as the forcing mechanism for the PDO (Davis 1976; Kumar and Wang 2015), the existence of the low-frequency component in the PDO variability is still consistent in that the stochasticity-inherent atmospheric variability can nudge the PDO to a particular phase over long periods of time, consistent with the idea of the ocean as a red noise integrator of the white noise atmospheric forcing (Frankignoul and Hasselmann 1977).

Having a conceptual framework that provides a basis for the notion for the existence of low-frequency variability of the PDO, we explore the possibility of defining an alternate PDO index that brings forth its lower-frequency

Corresponding author address: Dr. Arun Kumar, Climate Prediction Center, 5830 University Research Court, College Park, MD 20740.
E-mail: arun.kumar@noaa.gov

DOI: 10.1175/MWR-D-16-0080.1

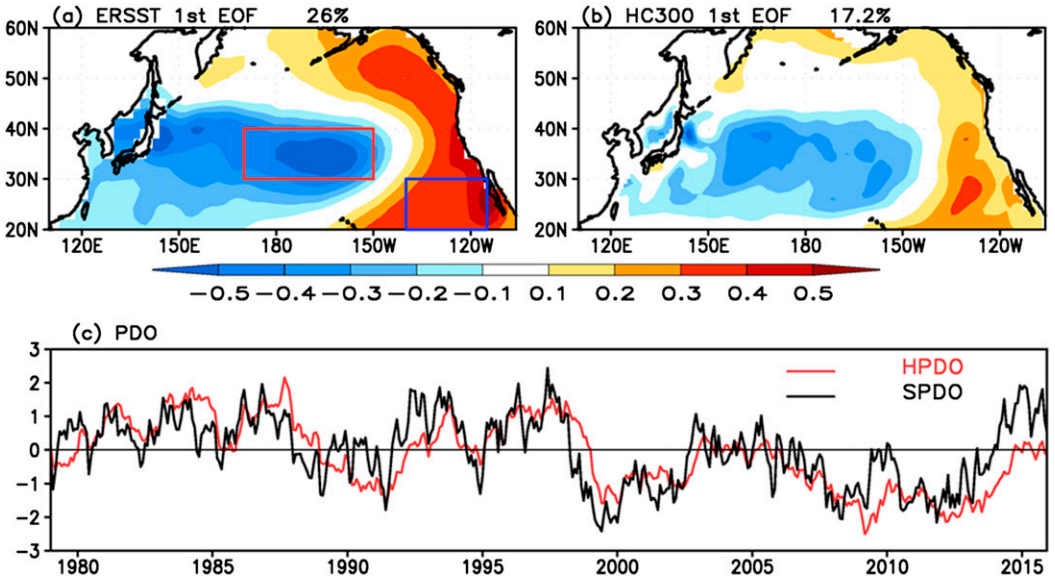

FIG. 1. Spatial structure of (a) the SST-based definition of PDO and (b) the HC300-based definition PDO. (c) Corresponding time series are shown for the SST-based PDO index (black) and the HC300-based PDO index (red).

component without relying on the time averaging of the PDO index defined based on SSTs. The feasibility of such an index may be possible, as in recent decades the ocean observing system has expanded to cover routine sampling of the upper oceans. Availability of real-time monitoring data throughout the upper oceans, due to evolution in the ocean observing system, allows one to explore the plausibility of developing a definition of the PDO index that brings forth the slowly varying elements of the characteristics of the PDO discussed above. Toward that, we propose a PDO index based on the heat content variability in the upper 300 m of the ocean, and supporting analysis is presented in this paper.

2. Data and methods

SST data in our analysis are from the Extended Reconstructed SST, version 3b (ERSST.v3b) (Smith et al. 2008), at a resolution of 2° × 2° latitude–longitude. SST anomalies (SSTA) are calculated based on its 1981–2010 climatology. Our definition for the SST-based PDO index is similar to that of Mantua et al. (1997). The SST PDO index is constructed by projecting SST anomalies onto the leading EOF of SSTA over the North Pacific (20°–60°N) after removing the global mean of SSTA. The 30-yr period from 1981 to 2010 is used in the EOF analysis. Hereafter, the SST-based PDO index is referred as SPDO.

Heat content in the upper 300 m (HC300) and subsurface temperature data are taken from the National Centers for Environmental Prediction (NCEP) Global Ocean Data Assimilation System (GODAS) analysis (Behringer and Xue 2004), a widely used ocean analysis product in the research community. The GODAS is based on the Geophysical Fluid Dynamics Laboratory (GFDL) Modular Ocean Model (MOM.v3) and a three-dimensional variational data assimilation scheme (3DVar). The model domain is from 75°S to 65°N and has a resolution of 1° by 1° and decreases to ⅓° in the north–south direction within 10° of the equator. The model has 40 levels with a 10-m resolution in the upper 200 m. The subsurface observations assimilated in GODAS include ocean temperature profiles from XBTs, CTDs, moored arrays, and more recently, Argo profiling floats. The GODAS dataset is available since 1979 for the monthly mean fields with resolution on a 1° × 1° horizontal. Similar to SPDO, we define a new index using HC300 as projection of HC300 anomalies onto its first EOF over the North Pacific (20°–60°N). Hereafter, this PDO index is referred as HPDO.

In this study, all anomalies are computed relative to 1981–2010 climatology and the analysis period is from 1979 to 2015.

3. Results

The spatial structures of SST-based PDO and HC300-based PDO are shown in Figs. 1a and 1b, and the corresponding time series are shown in Fig. 1c. In general, the spatial patterns of SPDO and HPDO share common

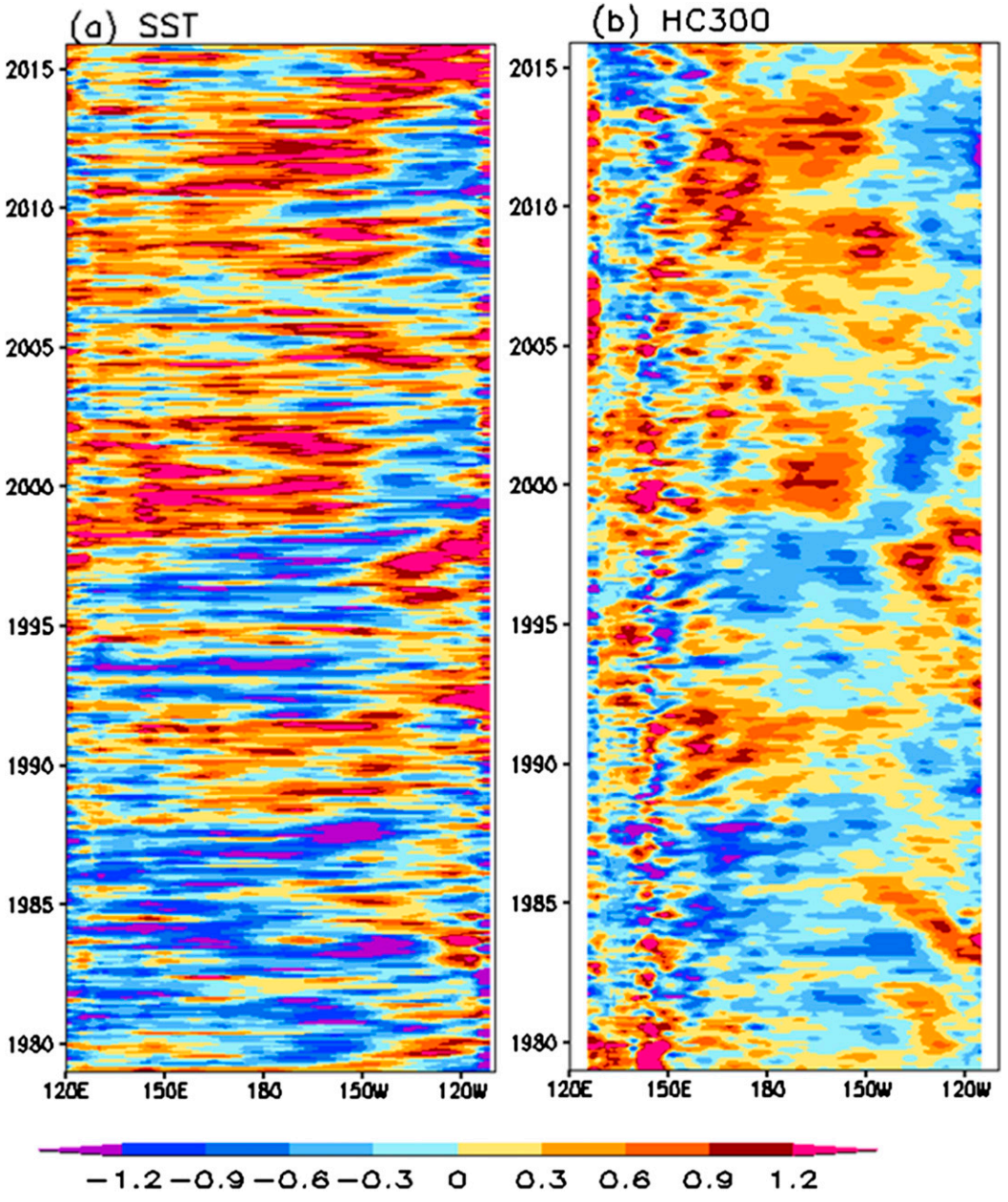

FIG. 2. Longitude–time cross sections of (a) SSTA and (b) HC300 anomalies (K) averaged between 30° and 40°N.

features with a center of largest loading in the east–west direction confined between 30° and 40°N, and extending from the eastern coast of Japan to over the central Pacific. A center of opposite polarity extends in the north–south direction along the western coast of North America. One difference between their spatial structures is that while for the SPDO the largest amplitude is along the coastal regions of North America, it is shifted farther away from the coast for the HPDO. Despite some differences, however, the similarities between the two patterns indicate that both approaches are identifying the same mode of variability.

It is the comparison of the corresponding time series that summarizes the major difference between the PDO indices defined based on SST or HC300. The month-to-month variability in the SPDO index is much larger than that for the HC300 index. This is to be expected as temporal variations in SSTs in response to the overlying atmospheric variability will occur on a faster time scale than the variability over the upper 300 m of the ocean. A faster time scale for SST variability compared to the variability in HC300 is confirmed in Fig. 2, where the temporal variations in SSTA and HC300 that averaged between 30°

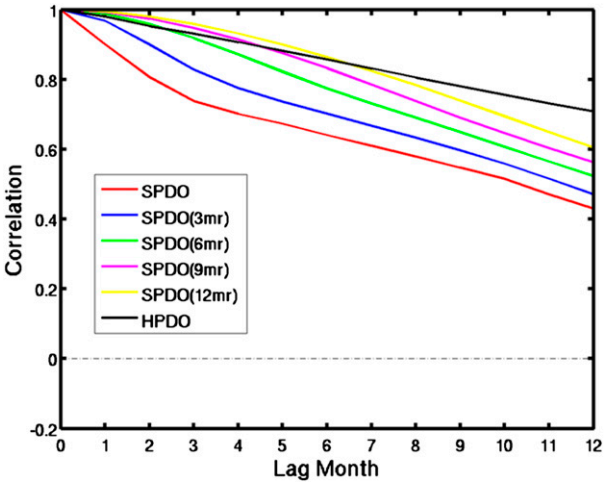

FIG. 3. Autocorrelations for the SPDO index (red) and HPDO index (black). Autocorrelations are based on corresponding time series shown in Fig. 1c. For the SPDO index, autocorrelations are also computed after smoothing the monthly SPDO time series with various monthly running (mr) means from 3 to 12 months.

and 40°N across the North Pacific are shown. Consistent with the PC time series in Fig. 1, the temporal variations in SST across the North Pacific are on a much faster time scale than that for HC300. Further, similar to the respective PDO indices in Fig. 1, a shift in the phase of the PDO around 1999 is also apparent.

Differences in the characteristic time scale of variations between SPDO- and HPDO-based indices are easily discerned based on the analysis of autocorrelation for the respective time series (Fig. 3). For an HPDO index, while the autocorrelation for monthly values at 6 (12) months is ~0.85 (0.75), for the SPDO index the corresponding values are ~0.6 (0.4), implying much more rapid temporal variations. It is only when the autocorrelation of the SPDO index is done on a time series that has a 12-month smoothing that the autocorrelation for the SPDO- and HPDO-based indices is comparable. This correspondence also implies that the HPDO index provides a natural way to filter out the faster time-scale variations that are inherent in the SST-based PDO index.

The correspondence between the autocorrelation for the HPDO and for the 12-month time-smoothed SPDO index is confirmed in Fig. 4 where a general correspondence between the two time series is evident. Both indices are dominated by a preponderance to be in the positive phase prior to 1999 and then switch to a negative phase after 1999. The shift in the phase of the PDO index around 1999 is consistent with a similar shift in the other facets of the climate system around the same time; for example, precipitation increases in western Pacific (Zhang et al. 2012) accompanied by a freshening of upper oceans (Durack and Wijffels 2010); a change in the west–east gradient in the thermocline in equatorial tropical Pacific (Kumar and Hu 2014) and an enhancement in the intensity of trades; and an increase in ocean heat content and sea surface height in the western Pacific (Merrifield 2011).

Although there is a good degree of consistency between the HPDO and the smoothed SPDO index, there are also periods when either the amplitude or the tendency of change in the amplitude between the two can differ significantly. After the peak of the 1982/83 El Niño and its transition into La Niña conditions, while the SPDO index started to decline, the HPDO index maintained its upward trend (Fig. 4). There are also brief periods, for example, around 1992, when the SPDO index turned positive, while the HPDO index stayed in negative territory. Within an envelope of a general agreement between HPDO and smoothed SPDO, occasional episodes of discrepancy are to be expected and may depend on the sequence and the amplitude of atmospheric forcing and of tropical ENSO variability, and the manner in which the SST and the upper ocean as a whole respond to them.

Previous studies have documented the connection between PDO and ENSO SST variability in the equatorial tropical Pacific (Newman et al. 2016). This connection between SST variability in the North Pacific and the equatorial Pacific Ocean basin is through the atmospheric bridge whereby in response to the ENSO SST, atmospheric anomalies over the Pacific–North American (PNA) region (Trenberth et al. 1998) lead to SST anomalies that project on the spatial structure of the SPDO (Alexander 1990; Lau and Nath 1994; Alexander 1992). The connection, however, is not very robust, and on a monthly time scale, the temporal anomaly correlation between the SPDO and the ENSO SST index is only about 0.4 (Wen et al. 2012; Kumar et al. 2013). This is consistent with the fact that, on average, ENSO SST variability explains about 30% of the monthly mean atmospheric variability over the PNA region (Hoerling and Kumar 2002; Kumar et al. 2007) while the rest is associated either with the stochastic atmospheric variability or could be associated with other external forcings. Given that the connection between the SPDO and ENSO SST index has been explored previously, we repeat the analysis to explore (and to contrast) ENSO's relationship with the HPDO index.

The lead–lag correlation between the Niño-3.4 SST and the two PDO indices is shown in Fig. 5. The maximum lead–lag correlation between the monthly Niño-3.4 SST index and the SPDO index is ~0.4, and further, its structure is quite symmetric. Low correlation between the two indices is consistent with previous results (Wen et al. 2012; Kumar et al. 2013) and is indicative of

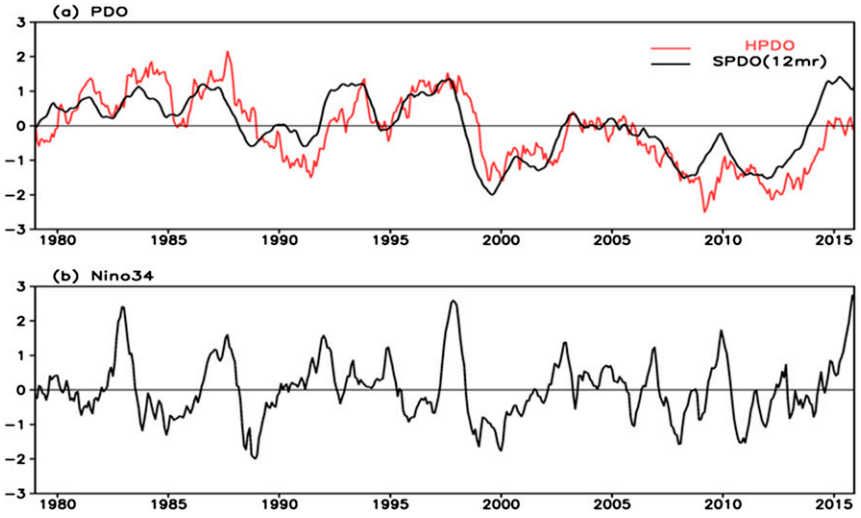

FIG. 4. (a) The HPDO index (red) and the 12-month running mean of the SPDO index (black). (b) The Niño-3.4 SST index.

the fact that a majority of SPDO variability on a monthly time scale is not constrained by the tropical Pacific ENSO variability.

In contrast to the correlation with the SPDO index, the correlation with the HPDO (red line) is asymmetric with a maximum value of 0.3 when HPDO lags ENSO by seven months. This lag in the maximum correlation is because of the downward propagation of temperature anomalies owing to the seasonal variation in the mixed layer.

An example of downward propagation of temperature anomalies is shown in Fig. 6 where a time–depth cross section of ocean temperature averaged between 30°–40°N and 170°E–150°W for 2008–12 is shown. This spatial domain for averages corresponds to the maximum center of variation explained by the PDO pattern (Fig. 1a, red box).

The temporal evolution of ocean temperature anomalies gives a clear indication of their origin at the surface of the ocean and subsequent downward penetration into the deeper ocean. The time scale of the downward propagation of temperature anomalies is associated with the annual cycle of the mixed layer depth that is deepest (shallowest) during boreal winter (summer). To highlight this, the time evolution in the mixed layer depth is also superimposed (Fig. 6, black line), where the mixed layer depth is defined as the depth at which the density changes by 0.125 kg m^{-3} from its surface value (Huang et al. 2010).

With the deepening of the mixed layer during boreal winter due to enhanced vertical mixing, the surface ocean temperature anomalies also propagate downward. Further, with the shoaling of the mixed layer during summer months an upward propagation of temperature anomalies is also evident. This downward propagation of temperature anomalies during boreal winter and their upward propagation during summer is a feature that has been referred to as the reemergence mechanism (Namias and Born 1974; Alexander 1990; Newman et al. 2016). A coherent vertical evolution of temperature anomalies from surface to deeper ocean also lends credibility of our attempt to define PDO as a vertical integral of temperature variability in the upper ocean.

As a further confirmation of downward propagation of temperature anomalies associated with ENSO, we show lead–lag correlation of subsurface temperature

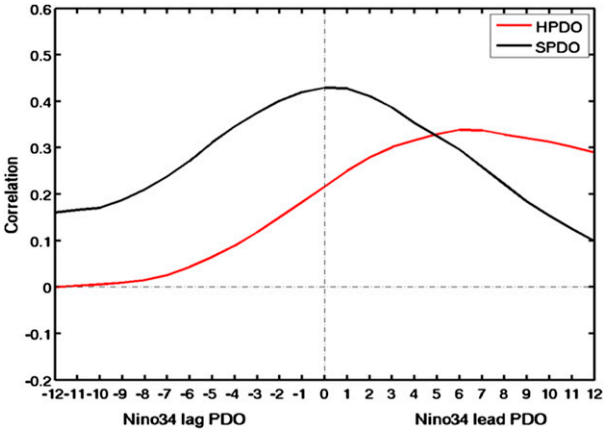

FIG. 5. Lead–lag correlation between the Niño-3.4 SST index and the SPDO index (black), and the Niño-3.4 SST index and the HPDO index (red).

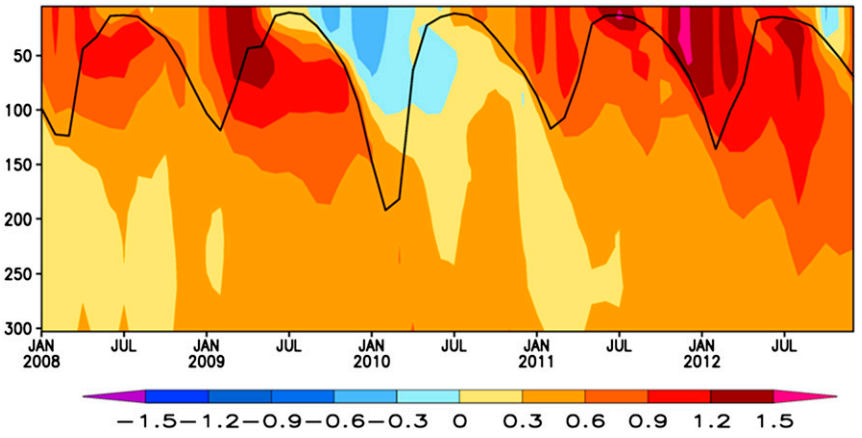

FIG. 6. Evolution of the ocean temperature anomaly (K) from the surface to 300 m averaged over 30°–40°N, 170°E–150°W (red box shown in Fig. 1a) from January 2008–December 2012. Black line denotes the temporal evolution of the mixed layer depth.

variability with the Niño-3.4 SST index at different ocean depths (Fig. 7). The lead–lag correlations are shown for ocean temperatures averaged over two locations corresponding to maximum centers of variance explained by the PDO pattern (see boxes in Fig. 1a).

For both locations, when the maximum in the temporal anomaly correlation between the Niño-3.4 SST index and ocean temperature occurs, the lead time increases with depth. For example, consistent with Fig. 5, at the surface the largest correlation occurs when the Niño-3.4 SST index leads the temperature anomaly by 1–2 months. On the other hand, at a depth of 120 m, the largest negative (positive) correlation over the western (eastern) box occurs when the Niño-3.4 SST index leads by ~9 (12) months. These results are consistent with the 7-month ENSO-leading HPDO relationship shown in Fig. 5, because as HC300 is a vertical integral of ocean temperature over the upper 300 m, the delay in HC300 will be some average of delay in ocean temperature at the surface and deeper with a weighted average of variability at respective depths. Beyond this mechanistic explanation for why there is a small lead–lag relationship between the Niño-3.4 SST index and SPDO, however, a longer lead for Niño-3.4 and the HPDO index, the latter may also be indicative of the influence of the North Pacific oceanic variability in modulating ENSO. As discussed in section 4, one such mechanism is via a shallow ocean pathway that allows PDO to influence ENSO activity through ocean subduction (McCreary and Lu 1994; Gu and Philander 1997; Yu et al. 2000; Alexander et al. 2006; Liu 2012).

For the discussion in the context of Fig. 4 we noted that there are occasions when the PDO index depicted by the SPDO or by the HPDO have periods of discrepancy when either the amplitude or the tendency of change in the amplitude between the two can differ. As noted earlier, this is to be expected and may be a result of a complex interplay between (i) seasonality of the

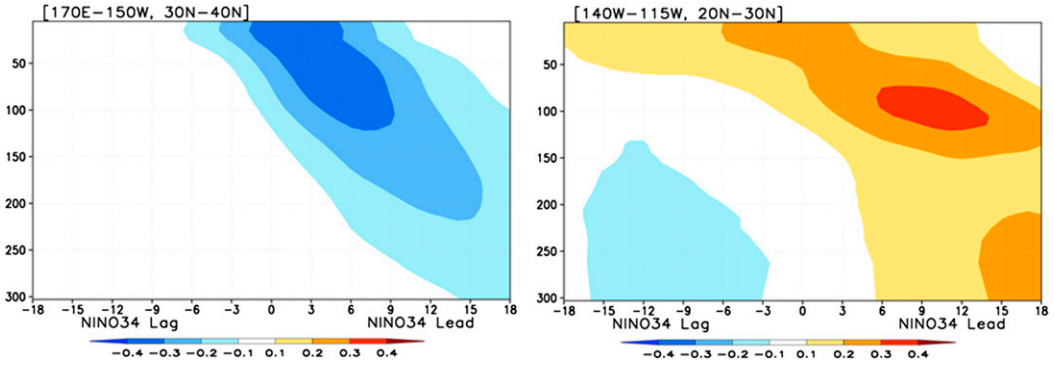

FIG. 7. Lead–lag correlation between the Niño-3.4 SST index and subsurface temperature anomaly at different depths averaged over (left) 30°–40°N, 170°E–150°W and (right) 20°–30°N, 140°–115°W. These two regions are shown in Fig. 1a as red and blue boxes, respectively.

mixed layer that determines the downward propagation of surface ocean temperature anomalies, (ii) timing of individual ENSO events, and further (iii) the temporal sequences of ENSO events.

4. Summary and discussion

In this analysis we presented an alternative approach to define the PDO variability in the North Pacific to supplement the traditional definition of the PDO based on SST variability. The alternative definition is based on the variability in the heat content over the upper 300 m of the ocean. Although a definition based on heat content would not have been possible prior to routine observations of ocean temperature in deeper oceans, with the evolution of the ocean observing system, such an approach is now feasible. Further, based on the current generation of ocean reanalysis products, the HC300-based definition of the PDO can at least be extended back to 1980, and in some instances, there are ocean reanalyses that may also allow its extension to earlier periods (see Carton and Giese 2008; Balmaseda et al. 2013). However, we note that the realism of the HC300 index based on those reanalyses would need to be carefully assessed. This is because of a lack of subsurface ocean observations, and also because of the possible degradation in the quality of surface forcing (e.g., surface wind stress) as the ocean analysis is extended farther back in time. Another desirable trait that the ocean reanalysis that extends over a longer period may lack (e.g., Carton and Giese 2008) is their update in real time, and consequently, it does not allow for an extension of the HPDO in real time.

We would also like to point out that it is not unprecedented to have multiple definitions, and indices, characterizing the same phenomenon, with alternate indices finding different utilities. For example, the North Atlantic Oscillation (NAO) is defined in multiple ways: a difference of atmospheric pressure at sea level between two geographical locations over the North Atlantic (and with the caveat that several choices for different geographical locations also exist); another definition of NAO is based on the empirical orthogonal function (EOF) analysis of sea level pressure or of upper-level heights; and even here, choices of the region over which EOF is performed are also not unique.

Some other complementary aspects of HC300-based definition of PDO (i.e., the HPDO) also include the following:

- By construct, the time evolution of HPDO is on a lower time scale, and as such, temporal evolution in HPDO provides a natural way to view the slower variations in the SST-based PDO index. Also, temporal variations in the HPDO better convey the decadal variability that is inherent in the definition, and the concept of the PDO.
- Ocean temperature variability associated with PDO not only occurs at surface, but due to ocean mixing, and seasonal cycles in the evolution of the oceanic mixed layer, also extends to deeper oceans (Wang et al. 2012b). HPDO, therefore, is able to encapsulate a more integrated view in the evolution of PDO.
- It is the subsurface ocean temperature anomalies associated with the PDO that might be related to the decadal modulation of ENSO variability in the equatorial tropical Pacific via a shallow ocean pathway that allows PDO to influence ENSO activity through ocean subduction (McCreary and Lu 1994; Gu and Philander 1997; Yu et al. 2000; Alexander et al. 2006; Liu 2012). By incorporating temperature variability in deeper oceans, the HPDO index may provide a better indicator for analyzing and documenting such influences.

Given the possibility that the HPDO index can supplement its surface-based counterpart in documenting variability associated with the Pacific decadal oscillation, we plan to incorporate it as part of routine ocean monitoring products at the Climate Prediction Center. Both of the definitions, however, are based on the EOF analysis of the oceanic variability in the North Pacific, and as such, do not add to further insights into physical causes of the PDO variability. Going beyond the observational analysis presented in this paper, one can also envision exploring physical interactions between the HPDO and its possible connections with the low-frequency variability in ENSO.

Acknowledgments. We thank comments by two anonymous reviewers and by the editor. We also thank NOAA's Climate Program Office and Climate Observation Division for their support. Editorial assistance by Janie Nall is also appreciated.

REFERENCES

Alexander, M. A., 1990: Simulation of the response of the North Pacific Ocean to the anomalous atmospheric circulation associated with El Niño. *Climate Dyn.*, **5**, 53–65, doi:10.1007/BF00195853.

——, 1992: Midlatitude atmosphere–ocean interaction during El Niño. Part I: The North Pacific Ocean. *J. Climate*, **5**, 944–958, doi:10.1175/1520-0442(1992)005<0944:MAIDEN>2.0.CO;2.

——, and Coauthors, 2006: Extratropical atmosphere–ocean variability in CCSM3. *J. Climate*, **19**, 2496–2525, doi:10.1175/JCLI3743.1.

Balmaseda, M. A., K. Morgensen, and A. T. Weaver, 2013: Evaluation of the ECMWF ocean reanalysis system ORAS4. *Quart. J. Roy. Meteor. Soc.*, **139**, 1132–1161, doi:10.1002/qj.2063.

Behringer, D. W., and Y. Xue, 2004: Evaluation of the global ocean data assimilation system at NCEP: The Pacific Ocean. Preprints, *Eighth Symp. on Integrated Observing and Assimilation Systems for Atmosphere, Oceans, and Land Surface*, Seattle, WA, Amer. Meteor. Soc., 2.3. [Available online at https://ams.confex.com/ams/84Annual/techprogram/paper_70720.htm.]

Carton, J. A., and B. S. Giese, 2008: A reanalysis of ocean climate using Simple Ocean Data Assimilation System (SODA). *Mon. Wea. Rev.*, **136**, 2999–2017, doi:10.1175/2007MWR1978.1.

Davis, R. E., 1976: Predictability of sea surface temperature and sea level pressure anomalies over the North Pacific Ocean. *J. Phys. Oceanogr.*, **6**, 249–266, doi:10.1175/1520-0485(1976)006<0249:POSSTA>2.0.CO;2.

Durack, P. J., and S. E. Wijffels, 2010: Fifty-year trends in global ocean salinities and their relationship to broad-scale warming. *J. Climate*, **23**, 4342–4362, doi:10.1175/2010JCLI3377.1.

Frankignoul, C., and K. Hasselmann, 1977: Stochastic climate models. Part II: Application to sea-surface temperature anomalies and thermocline variability. *Tellus*, **29A**, 289–305, doi:10.1111/j.2153-3490.1977.tb00740.x.

Gu, D., and S. G. H. Philander, 1997: Interdecadal climate fluctuations that depend on exchanges between the tropics and extratropics. *Science*, **275**, 805–807, doi:10.1126/science.275.5301.805.

Hoerling, M. P., and A. Kumar, 2002: Atmospheric response patterns associated with tropical forcing. *J. Climate*, **15**, 2184–2203, doi:10.1175/1520-0442(2002)015<2184:ARPAWT>2.0.CO;2.

Huang, B., Y. Xue, D. Zhang, A. Kumar, and M. J. McPhaden, 2010: The NCEP GODAS ocean analysis of the tropical Pacific mixed layer heat budget on seasonal to interannual time scales. *J. Climate*, **23**, 4901–4925, doi:10.1175/2010JCLI3373.1.

Kumar, A., and Z.-Z. Hu, 2014: Interannual and interdecadal variability of ocean temperature along the equatorial Pacific in conjunction with ENSO. *Climate Dyn.*, **42**, 1243–1258, doi:10.1007/s00382-013-1721-0.

——, and H. Wang, 2015: On the potential of extratropical SST anomalies for improving climate predictions. *Climate Dyn.*, **44**, 2557–2569, doi:10.1007/s00382-014-2398-8.

——, B. Jha, Q. Zhang, and L. Bounoua, 2007: A new methodology for estimating the unpredictable component of seasonal atmospheric variability. *J. Climate*, **20**, 3888–3901, doi:10.1175/JCLI4216.1.

——, H. Wang, W. Wang, Y. Xue, and Z.-Z. Hu, 2013: Does knowing the oceanic PDO phase help predict the atmospheric anomalies in subsequent months? *J. Climate*, **26**, 1268–1285, doi:10.1175/JCLI-D-12-00057.1.

Lau, N. C., and M. J. Nath, 1994: A modeling study of the relative roles of tropical and extratropical SST anomalies in the variability of the global atmosphere–ocean system. *J. Climate*, **7**, 1184–1207, doi:10.1175/1520-0442(1994)007<1184:AMSOTR>2.0.CO;2.

Liu, Z., 2012: Dynamics of interdecadal climate variability: A historical perspective. *J. Climate*, **25**, 1963–1995, doi:10.1175/2011JCLI3980.1.

Mantua, N. J., S. R. Hare, Y. Zhang, J. M. Wallace, and R. C. Francis, 1997: A Pacific interdecadal climate oscillation with impacts on salmon production. *Bull. Amer. Meteor. Soc.*, **78**, 1069–1079, doi:10.1175/1520-0477(1997)078<1069:APICOW>2.0.CO;2.

McCreary, J. P., Jr., and P. Lu, 1994: Interaction between the subtropical and equatorial ocean circulations: The subtropical cell. *J. Phys. Oceanogr.*, **24**, 466–497, doi:10.1175/1520-0485(1994)024<0466:IBTSAE>2.0.CO;2.

Merrifield, M. A., 2011: A shift in western tropical Pacific sea level trends during the 1990s. *J. Climate*, **24**, 4126–4138, doi:10.1175/2011JCLI3932.1.

Namias, J., and R. M. Born, 1974: Further studies of temporal coherence in North Pacific sea surface temperatures. *J. Geophys. Res.*, **79**, 797–798, doi:10.1029/JC079i006p00797.

Newman, M., and Coauthors, 2016: The Pacific Decadal Oscillation, revisited. *J. Climate*, **29**, 4399–4427, doi:10.1175/JCLI-D-15-0508.1.

Smith, T. M., R. W. Reynolds, T. C. Peterson, and J. Lawrimore, 2008: Improvements to NOAA's historical merged land-ocean surface temperature analysis (1880–2006). *J. Climate*, **21**, 2283–2296, doi:10.1175/2007JCLI2100.1.

Trenberth, E. K., G. W. Branstrator, D. Karoly, A. Kumar, N.-C. Lau, and C. Ropelewski, 1998: Progress during TOGA in understanding and modeling global teleconnections associated with tropical sea surface temperatures. *J. Geophys. Res.*, **103**, 14 291–14 324, doi:10.1029/97JC01444.

Wang, H., A. Kumar, W. Wang, and Y. Xue, 2012a: Influence of ENSO on Pacific decadal variability: An analysis based on the NCEP Climate Forecast System. *J. Climate*, **25**, 6136–6151, doi:10.1175/JCLI-D-11-00573.1.

——, ——, ——, and ——, 2012b: Seasonality of the Pacific decadal oscillation. *J. Climate*, **25**, 25–38, doi:10.1175/2011JCLI4092.1.

Wen, C., Y. Xue, and A. Kumar, 2012: Seasonal prediction of North Pacific SSTs and PDO in the NCEP CFS hindcasts. *J. Climate*, **25**, 5689–5710, doi:10.1175/JCLI-D-11-00556.1.

——, A. Kumar, and Y. Xue, 2014: Factors contributing to uncertainty in Pacific decadal oscillation index. *Geophys. Res. Lett.*, **41**, 7980–7986, doi:10.1002/2014GL061992.

Yu, J.-Y., W. T. Liu, and C. R. Mechoso, 2000: The SST anomaly dipole in the northern subtropical Pacific and its relationship with ENSO. *Geophys. Res. Lett.*, **27**, 1931–1934, doi:10.1029/1999GL011340.

Zhang, L., A. Kumar, and W. Wang, 2012: Influence of changes in observations on precipitation: A case study for the Climate Forecast System Reanalysis (CFSR). *J. Geophys. Res.*, **117**, D08105, doi:10.1029/2011JD017347.